

# **Adsorption of colour pigments from palm kernel oil onto biopolymer prepared from periwinkle shell waste**

## **Abstract**

The study was carried out to investigate the bleaching efficiency of chitosan for pigments removal from palm kernel oil (PKO). Chitosan was synthesized from periwinkle shell waste by chemical technique involving demineralization, deproteinization and deacetylation. The bleaching was carried out (batch process) at various adsorbent dosages (1.0-3.0 g). The bleaching adsorbents (Periwinkle Shell Powder, PSP and chitosan periwinkle shell powder, CPSP) were characterized using X-ray fluorescence (XRF) for their elemental composition, X-ray diffraction (XRD) for their mineral composition, scanning electron microscopy (SEM) for surface morphology and Fourier Transform Infrared (FTIR) was used to observe the presence of functional groups in the samples. The results obtained revealed alteration in the concentration (wt. %) and distribution of different compositional elements. The XRD analysis revealed pure crystalline character in CPSP attributed to the presence of aragonite at  $2\theta$  value of 29.2. The broad peak at  $3272.6\text{ cm}^{-1}$  and the absence of bands  $1744.4$ ,  $1628.8$ ,  $1461.1\text{ cm}^{-1}$  in PSP revealed forming and breaking of bonds in PSP and CPSP. The bleaching process was tested with four different adsorption isotherms (Langmuir, Freundlich, Temkin and Dubinin – Radushkevich (D-R). The PSP has the higher percentage bleaching efficiency (66.56) while CPSP has 47.05 using 1.0 g each of the biopolymer however  $1/n$  Freundlich isotherm constants which is an indication of adsorption intensity was higher in CPSP (3.4) compare with PSP (2.68). The adsorption process followed D-R in both CPSP and PSP ( $R^2$ ; 0.827 and 0.988 respectively) the mean free energies (E<sub>k</sub>/mol) of both CPSP and PSP (-35.71 and -12.90 respectively) were less than 8 kJ/mol suggesting physical adsorption.

Keywords: Palm kernel oil, Chitosan, Adsorption isotherm, Periwinkle shell waste, biopolymer

## **1. INTRODUCTION**

Chitin and chitosan are nitrogenous polysaccharides that compose of acetylglucosamine and glucosamine units. Both chitosan and chitin have exactly the same basic chemical structure

but differ only in the degree of deacetylation (i. e. deacetylation degree; DD) and their respective solubility in dilute acetic media. Chitosan is the only derivative that is soluble at a deacetylation degree above 40 % (Sorlier *et al.*, 2001). The second most abundant polymer in nature is chitin and occurs in nature as ordered crystalline microfibrils forming structural components in the exoskeleton of arthropods (Rinaudo, 2006). Chitosan has been described as a semi crystalline polymer in the solid state (Rinaudo, 2006). Chitosan is biologically renewable, biodegradable, biocompatible, non-antigenic, non-toxic (used in food industry) (Shanta *et al.*, 2015) and biofunctional (Malafaya *et al.*, 2007 ). Chitosan ( Fig. 1) is a natural polysaccharide that is synthesized from the partial deacetylation of chitin, a natural polymer made up of randomly distributed  $\beta$ -(1-4 linked D glucosamine and N- Acetyl-D-glucosamine that is found in the hard outer shells of crustaceans such as crabs, oyster, periwinkles and shrimps (Randy *et al.*, 2015, Tolamite *et al.* , 2000 ).

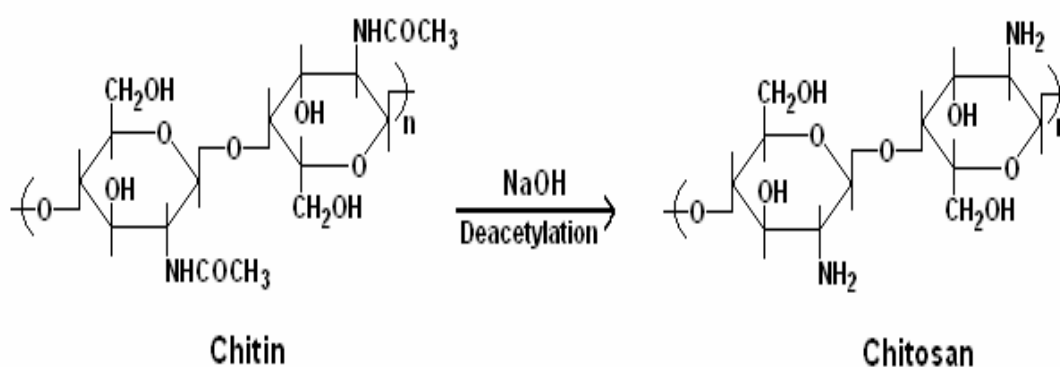


Fig1. Chemical structure of Chitin and chitosan

Chitosan has a fiber – like structure and of high molecular weight and similar to cellulose in structure but slightly different due to the amine ( $\text{-NH}_2$ ) group attached to carbon 2 position of chitosan instead of the hydroxyl ( $\text{OH}$ ) group found in the cellulose. Unlike the plant fibre, chitosan possesses a positive ionic charge which is responsible for its ability to chemically

bind with negative charged fats, lipids, cholesterol, metal ion, proteins and macromolecules (Li *et al.*, 1992). The ability of chitosan chemically form bond with negatively charged fats, lipids, and cholesterol and metal ions has made it effective and efficient for the bleaching of edible oils such as palm kernel oil. Chitosan is soluble in most mineral and organic acids due to the protonation of its amino groups though relatively stable in sulphuric acid solutions but insoluble at higher pH levels. Chitosan has been investigated to have other biological properties such as antimicrobial (Martins *et al.*, 2014) and antioxidant activities (Ngo *et al.*, 2014) and has many applications in area of biomedical and other industries (Heet *et al.*, 2017). Chitosan can be modified by chemical or physical processes in order to enhance the reactivity of the polymer or improve the sorption kinetics depending on the area of application (Guibal, 2004). The chemical modification improve its adsorption properties and to change the solubility properties of chitosan in water or acidic medium. This may include substitution reactions, chain elongation (cross-linking, graft copolymerization and polymer networks), and depolymerization (chemical, physical, and enzymatic) (Harish and Tharanathan 2007). Chitosan forms salt with inorganic and organic acids like glutamic acid, lactic acid, hydrochloric acid and acetic acid (Gavhane *et al.*, 2013).

Vegetable oils and fats are essential components of human diets. Nearly all oils produced in the world are of vegetable source (Guliyev *et al.*, 2018). The crude vegetable oils are mixture of different free fatty acids, mono- di- and triglycerides, phosphatides, glycolipids, pigments, sterols and tocopherols, flavonoids, tannins, and trace amounts of metals may also be present (Tilahun *et al.*, 2018). Nutritionally, vegetable oils are excellent sources of energy and important vehicles of liposoluble vitamins in the human body (Tonfack *et al.*, 2019).

The oil palm fruit yields two types of oil: palm oil from the fleshy mesocarp and palm kernel oil from the kernel. The two oils vary in composition and properties and as a result find rather different applications. Palm kernel oil is said to be the second most consumed lauric acid

group of oils similar in composition and properties to coconut oil (Poku, 2002). Palm kernel oil contains high content of saturated acids, lauric and myristic being the basic feature through which their principal uses were derived (Yerima *et al.*, 2018). Its low degree of unsaturation gives it high oxidative stability compared to other oils as it can be stored for longer period under normal condition than other vegetable oils (Knight, 2012). Palm kernel oil is widely used for industrial purposes in manufacturing of high quality soaps, vegetable oil and margarine. It is also used locally as body creams, cooking oils and medicinally as antidotes for poisoning and as surface protectants for minor wounds (Ekpa, 1995). It has also been used as feedstock in the production of biodiesel and as lubricant in the energy sector (Musa, 2010).

Bleaching is a critical step in the physical and chemical refining process of edible oils and selecting the optimal condition for the bleaching process depends on the quality and type of crude oil. Bleaching is not just declourization of edible vegetable oils but involve selective removal of pigments and impurities by the physical and chemical interaction of an adsorbent with an oil to improve its quality including the removal of trace metals such as copper (Cu), iron (Fe). The bleaching process is applied after degumming and neutralization in the chemical refining and it is more appropriately referred to as adsorption treatment (Guliyev *et al.*, 2018).

As a result of the increasing of world population, there is a growing demand for edible oil. The refining process is inevitably becoming the most essential step adopted by oil processors for producing edible oil with improving taste, appearance and increase the shelf life for fulfilling the high demand. Physical refining is extensively used in the vegetable oil industry (Biow Ing Sim *et al.*, 2018).

Periwinkle contributes adversely to the environmental management in the coastal regions, especially places where fishery appears to be a highly profitable business and periwinkle as

dominant products of shellfish farm. Such industry has a potential of serious problems about disposal of periwinkle shell waste and hence constitute a nuisance to the environment (Gil-Lim *et al.*, 2013). The presence of clay minerals, particularly silicon dioxide ( $\text{SiO}_2$ ) and aluminum oxide ( $\text{Al}_2\text{O}_3$ ), contributes to the high adsorptive property of periwinkle shell (Salawudeen *et al.*, 2007). The aim and objective of this study was to characterized and investigate the potential application of chitosan prepared from periwinkle shell powder for the removal of colour pigments from palm kernel oil.

## **2.0 MATERIALS AND METHOD**

### **2.1 Sample Collection and Materials**

Periwinkle shells were obtained in Warri (Rivers State) from the river side. Palm kernel oil was purchased in Auchi from a local producer in Auchi, Edo State. All reagents used were of analytical grade.

### **2.2 Methods**

#### **2.2.1 Preparation of periwinkle shell**

The shells were properly washed with hot water to remove the remaining fleshy materials and surface dirt and then air dried for five days. The shells were crushed and ground to powder form using a roller mill machine. The powdered sample was sieved into different particle sizes using sieve of (300, 250, 200, 150, 100  $\mu\text{m}$ ). The particle size of 100  $\mu\text{m}$  was stored and used for the study and labeled as periwinkle shell powder (PSP).

**2.2.2 Demineralization of periwinkle shell:** The sample (250 g) was weighed and then transferred into a 1000 mL beaker and 1M HCl (300 mL) solution was added and stirred thoroughly. The mixture was then heated in a water-bath at 100 °C for 60 min. The resulting mixture was filtered and washed with distilled water until a neutral pH was attained.

**2.2.3 Deprotenization of periwinkle shell:** Dried demineralized sample (200 g) was weighed into a beaker and 400 mL of 1 M NaOH (solid/liquid ratio 1:2 w/v) was added. The

mixture was heated using a thermostatically controlled hot plate with stirrer at 80 °C for 1 hr. The resultant mixture was filtered, washed with distilled water until a neutral pH was attained. Ethanol (100 mL) was added to the resulting solid sample and allowed to stand for 24 hr to decolourize the sample. The resulting chitin was filtered and dried in an oven at 80 °C for 1 hr.

**2.2.4 Deacetylation of periwinkle shell:** The resulting chitin from the deproteinization stage was deacetylated by adding 60 % NaOH solution to the sample and stirred thoroughly. The mixture was then washed until a neutral pH was attained and dried at 100 °C for 45 min. The drying was continued at 150 °C for another 20 min till the residue was free of moisture. The resulting powder which was the chitosan was labeled as CPSP (chitosan periwinkle shell powder).

### **2.3 Characterization PSP and CPSP**

The PSP and CPSP were characterized using XRF, FT-IR and SEM. X-Ray diffraction (XRD), the x ray diffraction method was used to determine the mineral compositions of the sample. X Ray Fluorescence was used to determine the chemical compositions of CPSP while Fourier Transform Infrared spectrometry (FT-IR) was used to investigate the presence of functional groups in the sample and Scanning Electron Microscopy (SEM) was used to observe the surface morphology of the sample.

### **2.4 Bleaching Process**

#### **2.4.1 Degumming**

This is the preliminary stage during bleaching of oils and the main objective of degumming is to remove the unwanted gums which can interfere with the stability of the oil in a larger scale production. Degumming was carried out by adding 0.1 % phosphoric acid (85 %) to the hot oil (30 g) in a beaker heated at 60 °C and was stirred thoroughly.

#### **2.4.2 Bleaching of Palm kernel Oil (PKO)**

The bleaching of palm kernel oil was carried out in a batch method. The degummed (PKO) (30 g) was weighed into a beaker and CPSP (1 g) was added, heated at 80 °C for 30 min. The mixture was filtered using a whatman No 1 filter paper as quickly as possible to prevent undesirable oxidation. This same procedure was carried out using 1.5, 2.0, 2.5 and 3.0 g and also carried out for PSP.

### **2.4.3 Analysis of Bleaching Performance**

The absorbance of palm kernel oil using both the CPSP and PSP was carried out using the UV-visible Spectrophotometer model 752. The bleaching efficiency of adsorbent was evaluated by monitoring the absorbance at 420 nm and expressed in terms of absorbance of light passing through the medium (PKO bleached with CPSP and PSP). The percentage colour reductions of the bleached oil was calculated using equation 1

$$\text{Bleaching Efficiency \%} = \frac{A_0 - A_t}{A_0} \times 100 \quad 1$$

Where,  $A_0$  = Absorbance of unbleached palm kernel oil (initial absorbance)

$A_t$  = Absorbance of bleached palm kernel oil at time t

## **2.5 Data analysis**

### **2.5.1 Adsorption isotherm studies**

The adsorption isotherm is important from both a theoretical and a practical point of view because the application of adsorption isotherm provide information describing the interaction between the adsorbate and the adsorbent of any system. There are several equations for analyzing experimental adsorption equation data. In the present study, Langmuir, Freundlich, Temkin and D-R isotherms were used to test the adsorption of colour pigments and other impurities from PKO onto CPSP and PSP.

### **2.5.2 Langmuir Isotherms**

The Langmuir isotherm has been employed to explain the adsorption of oil pigment and other minor oil solutes during oil processing. Langmuir, (1918) developed a model which describes gas adsorption. The model assumes that the adsorbate is bound to a fixed number of energetically equal, specific sites, each adsorbing one molecule with no interaction occurring between molecules on adjacent sites. The Langmuir isotherm has been applied to pigment adsorption from vegetable oil in the form of equation 2

$$\frac{X_e}{x/m} = \frac{1}{q_m K_L} + \frac{X_e}{q_m} \quad 2$$

Where  $x$  = amount of solute adsorbed,  $X_e$  is the amount of unadsorbed solute (the equilibrium concentration of adsorbate in solution mg/ L),  $m$  is the amount in grams of adsorbent used, ( $x/m$  is the adsorption capacity at the equilibrium solute concentration) ' $q_m$ ' maximum adsorption capacity (mg/g), and  $K_L$  is a constant of the intensity of the adsorption.

### 2.5.3 Freundlich Isotherms

Freundlich in 1926 developed an empirical equation that correlates the capacity of the adsorbent with the residual solute concentration using equation 3.

$$x/m = kC^n \text{ or } KC^{1/n} \quad 3$$

Where  $x$  = amount of solute adsorbed (mg),  $m$  = amount of adsorbent (g),  $c$  = amount of residual solute (concentration) (mg/L) at equilibrium. The Freundlich model is used to estimate the adsorption affinity of the sorbents towards the adsorbate (Jimoh *et al.*, 2011).  $K$  is a constant indicating adsorption capacity, and  $n$  is a constant of the energy of adsorption. Empirical data are evaluated for Freundlich behaviour by using the equation in its logarithmic form, as equation of a straight line (Achife and Ibemesi, 1989).

$$\log \frac{x}{m} = \log k + 1/n \log X_e \quad 4$$

### 2.5.4 Temkin Isotherm Model

Temkin isotherm is the early model describing the adsorption of hydrogen onto platinum electrodes within the acidic solutions (Temkin and Pyzhev, 1940). The isotherm contains a factor that explicitly taking into consideration the amount of adsorbent-adsorbate interactions. By ignoring the extremely low and large value of concentrations, the model assumes that heat of adsorption (function of temperature) of all molecules in the layer would decrease linearly rather than logarithmic with coverage which is attributed to adsorbate-adsorbate repulsions. It also assumes that adsorption is due to uniform distribution of binding energy contrary to Freundlich model. The amount of adsorbate is given as follows:

$$q_e = \left(\frac{RT}{b}\right) aC_e \quad 5$$

$$q_e = B \ln A + B \ln C_e \quad 6$$

$$B = \frac{RT}{b} \quad 7$$

$q_e$  (mg/g) and  $C_e$ (mg/g) are the amount of adsorbed pigments per unit weight of adsorbent and unadsorbed pigment at equilibrium respectively. A and B are the Temkin constants. The Temkin isotherm parameters were obtained by plotting  $q_e$  against  $\ln C_e$ . It would be worth noting that the constant B is related to heat of adsorption.

### 2.5.5 Dubinin- Radushkevich Isotherm Model

Dubinin – Radushkevich isotherm is generally applied to express the adsorption mechanism with a Gaussian energy distribution onto a heterogeneous surface (Dabrowski, 2001; Gunay *et al.*, 2007). The model has often successfully fitted high solute activities and the intermediate range of concentrations data well.

$$q_e = (q_s) \exp(-K_{ad}\epsilon^2) \quad 8$$

$$\ln q_e = \ln(q_s) - (K_{ad} \varepsilon^2) \quad 9$$

$q_e$  = amount of adsorbate in the adsorbent at equilibrium(mg/g);  $q_s$  = theoretical isotherm saturation capacity(mg/g);  $K_{ad}$  = Dubinin-Radushkevich isotherm constant ( $\text{mol}^2/\text{kJ}^2$ );  $\varepsilon$  = Dubinin – Radushkevich isotherm constant. The approach was usually applied to distinguish the physical and chemical adsorption of metal ions with its mean free energy (E kJ/mol) for removing a molecule from its location in the sorption space to the infinity which can be computed by the relationship (Dubinin, 1960; Hobson, 1969).

$$E = \left( \frac{1}{\sqrt{2B_{DR}}} \right) \quad 10$$

$B_{DR}$  is the isotherm constant

$$\varepsilon = RT \ln \left( 1 + \frac{1}{C_e} \right) \quad 11$$

Where  $R=8.314 \text{ J/molK}$ ;  $T$  = absolute temperature;  $C_e$ = adsorbate equilibrium concentration (mg/L). One of the unique features of the Dubinin – Radushkevich (DRK) isotherm model lies on the fact that it is temperature – dependent, which when adsorption data at different temperatures are plotted as a function of logarithm of amount adsorbed  $\ln q_e$  against  $\varepsilon^2$  the

square of potential energy. All suitable data will lie on the same curve, named as the characteristic curve (Foo *et al.*, 2010). The constant such as  $q_s$  and  $K_{ad}$  are determined from the appropriate plot using equation 8.

The mean free energy E (kJ/mol) which is defined as the free energy change when one mole of ion is transferred to the surface of the solid. Mean free energy was calculated using the equation 12

$$E \text{ (kJ/mol)} = (2k)^{-1/2}$$

12

The value of  $E$  (kJ/mol) is used to estimate the kind of adsorption. If the value of  $E$  (kJ/mol) is in the range of 8-16 kJ/mol, the adsorption type is explained by ion-exchange, if  $E$  (kJ/mol) is less than 8 ( $E < 8$ ) the adsorption type is due to physisorption as a result of weak Van der Waal forces of attraction and if  $E$  greater than 8 ( $E > 8$ ) the adsorption type is chemical adsorption.

## 2.6 RESULTS AND DISCUSSION

### 2.6.1 Characterization of CPSP and RPSP

#### 2.6.2 Scanning Electron Microscopy (SEM)

The plate 1(a) shows the surface topography of RPSP and (b) CPSP as revealed by scanning electron microscopy. The result showed that most of the impurities and molecules have been leached with respect to CPSP while RPSP surface morphology revealed high degree of roughness due to tiny particles occupying most of the surface pores and large cavities were observed between the irregular, long needle-like and stony shape solids which also appeared more clearly and with less degree of roughness in CPSP surface morphology.

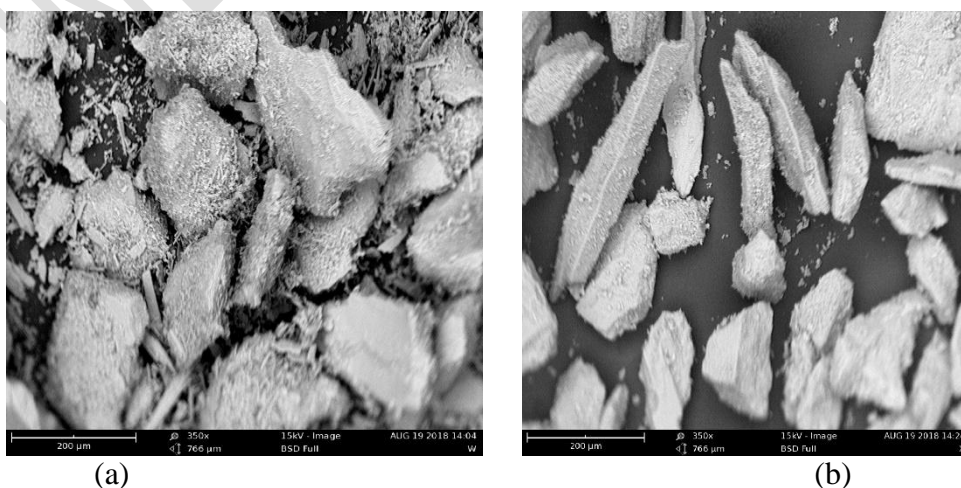


Plate 1: Scanning Electron Microscopy (SEM) morphology of (a) RPSP (b) CPSP

### 2.6.3 Fourier Transform Infrared (FT-IR) Analysis

Fig 2 shows the FT-IR spectrum of PSP while the absorption bands were presented in table 1. The peaks at 3280.1, 1304.6 and 1028.7  $\text{cm}^{-1}$  were due to the presence of hydroxyl group (OH) intermolecularly H-bonded. The absorption bands at 2922.2, 1543.1 and 2855.1  $\text{cm}^{-1}$  resulted as a result of the presence of CH stretching while the peaks at 1744.4 was the characteristic band of carbonyl group C=O stretching vibrations while the peak at 1461.1  $\text{cm}^{-1}$  resulted from carbonate ions from calcium carbonate the peak that appeared at 1397.8 was due to  $\text{CO}_3^{2-}$  stretching band and the absorption peak at 1028.7  $\text{cm}^{-1}$  was due to the stretching vibrations of Si- O-Si open chain. There was no indication of the presence of an aromatic ring due to the absence of the four bands in the 1600 to 1450  $\text{cm}^{-1}$  region and absence of bands in the 900 to 675  $\text{cm}^{-1}$  region.

Fig 4 shows the FT-IR spectrum of CPSP while the absorption bands were presented in table 2. Pawlak and Mucha (2003) reported that the FT-IR analysis of chitosan was based on the identification of bands and its vibrations. The presence of a broad OH stretch at 3272.6  $\text{cm}^{-1}$  indicated the characteristic band expected from  $\text{CO}_2\text{H}$  function in the sample. The peak at 2929.7  $\text{cm}^{-1}$  suggested the presence of CH stretch from alkyl group, while the absorption band at 1636.3  $\text{cm}^{-1}$  was the characteristic band due to an amide group in the CPSP. However, the absorption band at 1408.9  $\text{cm}^{-1}$  showed the presence of CH bending. The band at 1338.1  $\text{cm}^{-1}$  showed the presence of amide III group. The appearance of absorption band at 1148.0  $\text{cm}^{-1}$  showed the presence of C-O-C while the peak at 928.1  $\text{cm}^{-1}$  indicated the presence of C-O-C bending in the sample. The absorption peak at 1077.2  $\text{cm}^{-1}$  is an indication of CO stretching group. The appearance of bands at 760.4 and 704.5  $\text{cm}^{-1}$  indicated NH bending. The absorption peak at 995.2  $\text{cm}^{-1}$  was due to CH bending (out of plane wagging) while the peak at 861.0  $\text{cm}^{-1}$  was due to CH deformation (out of plane wagging).

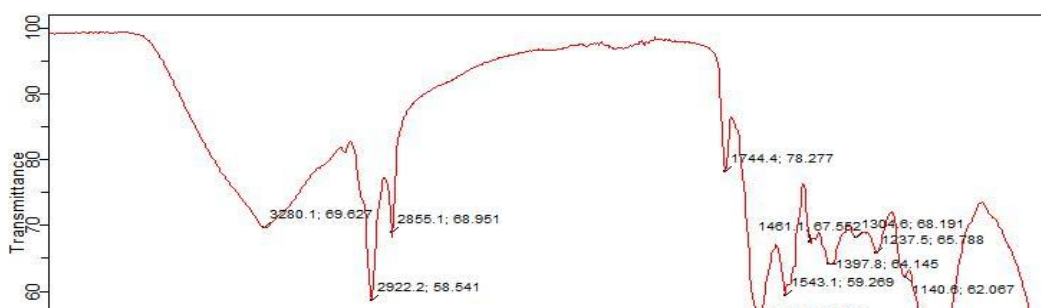


Fig. 2. FT-IR spectrum of PSP

Table 1. Absorption bands of RPSP

Absorption band (cm <sup>-1</sup> )	Functional groups
3280.1	OH intermolecularly (H-bonded)
2922.2	CH stretching
2855.1	CH <sub>2</sub> asymmetric
1744.4	C=O asymmetric
1628.8	C=O stretching vibrations
1543.1	OH (water of crystallization)
1461.1	Carbonates in CaCO <sub>3</sub>
1397.8	CO <sub>3</sub> <sup>-2</sup> in CaCO <sub>3</sub>
1304.6	OH group bonded to aliphatic compound
1237.5	C-O (carboxylic)
1140.6	OH group
1028.7	stretching vibration Si- O-Si open chain

The absorption band at 1394.0 cm<sup>-1</sup> suggested the presence of amide III while the absorption peak at 1066.0 cm<sup>-1</sup> revealed the presence of – C-O-C- due to glycoside linkage (Pawlak and Mucha 2003) and the presence of absorption band at 1021.3 cm<sup>-1</sup> indicated the presence of NH<sub>2</sub> (amino) group. The broad peak at 3272.6 cm<sup>-1</sup> and the absence of bands 1744.4, 1628.8, 1461.1 cm<sup>-1</sup> in CPSP showed clearly the difference between the PSP and CPSP.

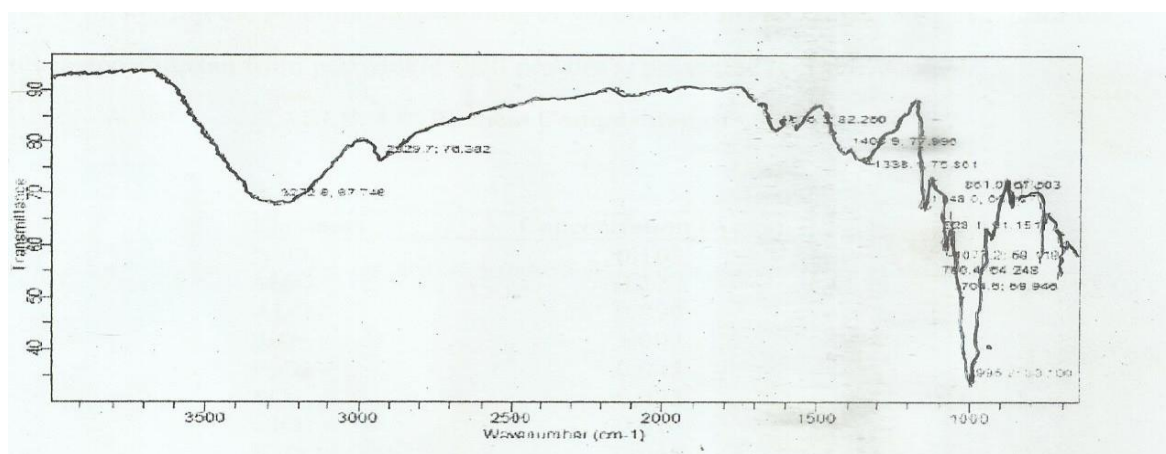


Fig. 3: FT-IR spectrum of CPSP

Table 2. Absorption bands of CPSP

Absorption bands (cm <sup>-1</sup> )	Functional groups
3272.6	O-H stretching
2829.7	C-H stretching
1636.3	NH <sub>2</sub> (amide) group,
1408.9	CO stretching of acetyl group
1338.1	C-H bending
1148.0	Amide III
1077.2	C-O-C bending
928.1	C-O stretching
760.4, 704.5	C-O bending
995.2	N-H bending
861.0	C-H bending (out of plane)
	C-H deformation (out of plane)

#### 2.6.4 X-ray Diffraction Result

The x-ray diffraction is a synthesis instrument used for the identification of crystalline phases of inorganic compound. The spectra obtained from the XRD as shown in fig. 5a and 5b revealed the characteristics mixture of crystalline and amorphous solid particles in PSP while CPSP exhibited a very single strong crystalline character and this was revealed at  $2\theta$  values of 29.2, the peak is a characteristic of CaCO<sub>3</sub> (aragonite). It is an indication that the major

crystalline phase of CPSP is aragonite ( $\text{CaCO}_3$ ). It clearly showed the crystalline nature and phase composition of CPSP.

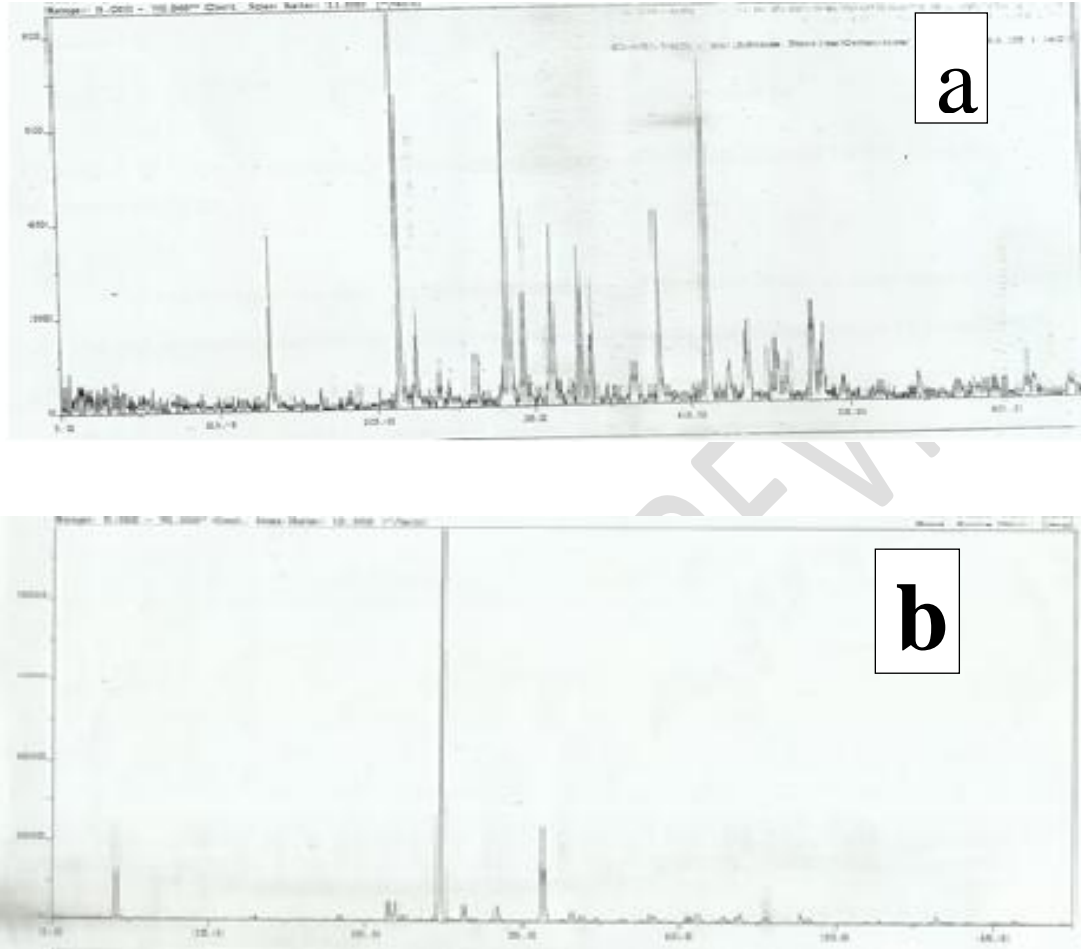


Fig. 4. X-Ray Diffraction spectra of (a) PSP and (b) CPSP

### 2.6.5 X-Ray Fluorescence (XRF)

The XRF result for the synthesized chitosan from oyster shell powder and the raw oyster shell powder were presented in the table 3. It was observed that the decrease in the concentration (wt. %) of CPSP showed that most of the minerals were leached during the process. The result showed that the synthesized CPSP has little or no trace of other element or impurities capable of affecting its potential in bleaching vegetable oil.

Table 3. X-Ray Fluorescence (XRF) of PSP and CPSP

Elements	Concentration (wt. %)	
	PSP	CPSP
Na <sub>2</sub> O	0.000	0.000
MgO	0.208	0.122
Al <sub>2</sub> O <sub>3</sub>	1.120	0.890
SiO <sub>2</sub>	3.109	3.002
P <sub>2</sub> O <sub>5</sub>	0.053	0.045
SO <sub>3</sub>	0.151	0.075
Cl	0.019	0.014
K <sub>2</sub> O	0.097	0.088
CaO	94.19	84.95
TiO <sub>2</sub>	0.032	0.000
Cr <sub>2</sub> O <sub>3</sub>	0.003	0.003
Mn <sub>2</sub> O <sub>3</sub>	0.049	0.032
Fe <sub>2</sub> O <sub>3</sub>	0.457	0.075
ZnO	0.000	0.000
SrO	0.510	0.438

### 2.6.6 Effect of Dosage

Figure 5 shows the bleaching efficiency of chitosan prepared from periwinkle shell powder (CPSP) and periwinkle shell powder (PSP). The result revealed that the adsorbent showed effect on the colour index of palm kernel oil. It was observed that the bleaching efficiency increase to an optimum value when 1.0 g of CPSP and PSP were used. Further increase in CPSP and PSP dosage did not show any effect on the colour of palm kernel oil as the percentage bleaching efficiency began to decrease with increase in quantity of the adsorbents. This might be as a result of the saturation of the available exchangeable sites on the adsorbent that inhibit further pigments adsorption onto its surface. It shows that adsorption equilibrium has been reached between the adsorbents-oil mixtures. The result revealed that PSP showed better colour pigments removal from PKO than CPSP based on their percentage bleaching efficiencies.

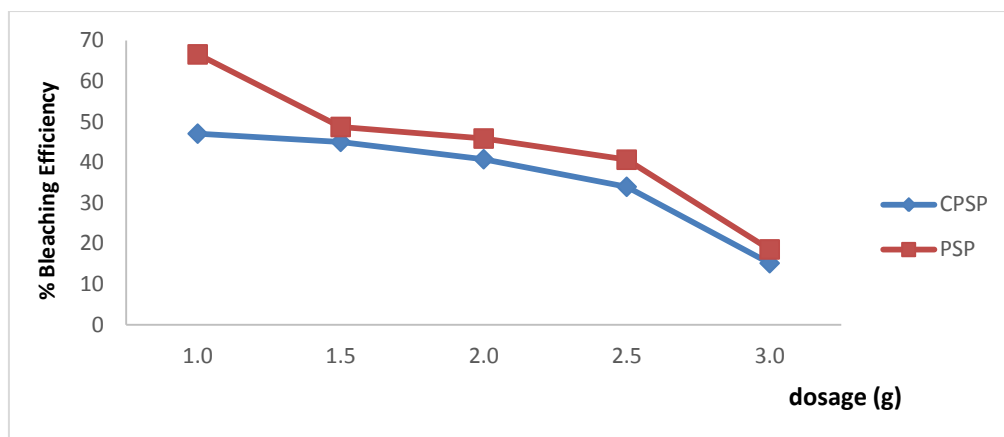


Figure 5. chart of % bleaching efficiency of both CPSP and PSP at various adsorbent dosage

### 2.6.7 Adsorption Isothermal Studies

The adsorption potential of PSP and CPSP was tested using four isotherm models (Langmuir, Freundlich, Temkin and Dubinin-Radushkevich) in order to understand the variation in the performance of the bleaching of PKO using PSP and CPSP. Isotherm constants are used as indicators to assess the efficiency of bleaching adsorbents. The equilibrium isotherms parameters were summarized in table 4. The values of constants of the isotherms were calculated from the slopes and intercepts of the plots as shown in figure 7. The result showed that Dubinin-Radushkevich isotherm was most suitable to explain the adsorption process in CPSP and PSP due to its high value of correlation coefficient ( $R^2$ ) of 0.827 and 0.988 respectively. However, the values of Langmuir dimensionless parameter ( $R_L$ ) were less than 1 ( $R_L < 1$ ) in both CPSP and PSP and indication of favourable adsorption. Freundlich parameter  $1/n$  values for CPSP and PSP were between 1 and 10 showing a favourable adsorption process. The mean free energy obtained for CPSP and PSP were less than 8 kJ/mol and this suggested that the adsorption process would proceed via physical adsorption in both CPSP and PSP.

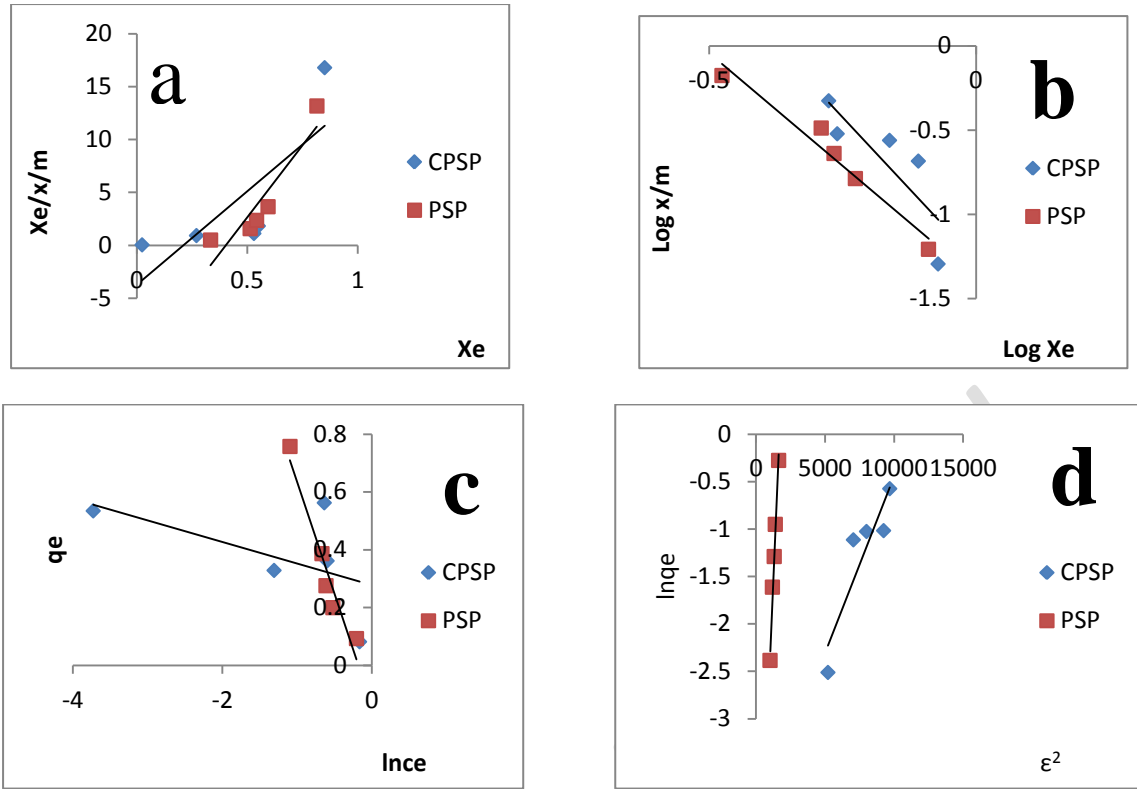


Fig. 6. Isotherm plots of (a) Langmuir, (b) Freundlich, (c) Temkin and (d) D-R

Table. 4 Adsorption isotherm constants for the bleaching of cottonseed oil with CPSP and PSP

	CPSP	PSP		
Langmuir	$q_{max}(mg/g)$	0.268	$q_{max}(mg/g)$	0.091
	$K_L(L/mg)$	4.741	$K_L(L/mg)$	2.479
	$R_L$	0.162	$R_L$	0.269
	$R^2$	0.607	$R^2$	0.848
Freundlich	$K_f(mg/g)$	9.478	$K_f(mg/g)$	7.101
	$1/n$	3.400	$1/n$	2.681
	$R^2$	0.701	$R^2$	0.959
Temkin	$B(mg/g)$	0.075	$B(mg/g)$	0.775
	$A (L/min)$	0.761	$A (L/min)$	0.582
	$R^2$	0.303	$R^2$	0.941
D-R	$q_m(mg/g)$	0.699	$q_m(mg/g)$	0.573
	$\beta(mol^2kJ^{-2})$	0.0004	$\beta(mol^2kJ^{-2})$	0.003
	$E(kJ/mol)$	-35.71	$E(kJ/mol)$	-12.90
	$R^2$	0.827	$R^2$	0.988

### 3.0 Conclusion

The raw periwinkle shell powder (PSP) showed stronger affinity for colour pigments and other impurities in palm kernel oil better than the chitosan prepared from periwinkle shell powder (CPSP). An obvious revelation that PSP is an excellent adsorbent for pigments removal from palm kernel oil. The adsorption process conformed to Dubinin-Radushkevich isotherm in both CPSP and PSP due to higher correlation coefficient (0.827 and 0.988). The free mean energies of both CPSP and PSP were less than 8 kJ/mol which showed that the adsorption occurred via physical adsorption. Therefore, since PSP is cheap, it could serve as an alternative to the more expensive conventional bleaching agents such as bentonite, activated charcoal etc. and more so PSP is readily available.

## References

- Achife, J. and Ibemesi, J (1989). Applicability of Freundlich and Langmuir Adsorption Isotherms in Bleaching of Rubber and Melon Seed Oils. *Journal of the American Oil Chemists' Society*, 66: 247-252.
- Biow Ing Sim, Halimah Muhamad, Oi Ming Lai, Faridah Abas, Chee Beng Yeoh, Imededdine Arbi Nehdi, Yih Phing Khor<sup>1</sup> and Chin Ping Tan (2018). New Insights on Degumming and Bleaching Process Parameters on The Formation of 3-Monochloropropane-1,2-Diol Esters and Glycidyl Esters in Refined, Bleached, Deodorized Palm Oil. *J. Oleo Sci.* 67, (4) 397-406
- Dubinin, M.M., (1960). The Potential Theory of Adsorption of Gases and Vapors for adsorbents with Energetically Non-Uniform Surface. *Chem. Rev.*, 60: 235–266.
- Dabrowski, A (2001). Adsorption- from theory to practice. *Adv. Colloid Interface Sci.* 93, 135-224.
- Ekpa, O. D (1995). Bio-inorganic constituents' and possible uses of the female fluorescence of the oil palm. *West African Journal Biol. Applied Chem.* 40: 13-18
- Foo, K.Y, Hameed, B.H (2010). Insight into the modeling of adsorption Isotherm systems, *Review Chemical Engineering Journal*, 156, 2-10.
- Freundlich, H., (1926). Colloid and capillary chemistry, *Metheum*, London,
- Guliyev, N. G, Ibrahimov, H. J, Alekperov, J. A, Amirov, F. A, Ibrahimova, Z. M(2018). Investigation of activated carbon obtained from the liquid products of pryolysis in sunflower oil bleaching process. *International Journal of Industrial Chemistry* 9, 277-284
- Gavhane, Y. N., Gaurav, A. S., Yadav, A. V (2013). Chitosan and its application: A review of literature. *International Journal of Research in Pharmaceutical and Biomedical.* 4, 312-331
- Gunay, A., Arslankaya, E., Tosun, I (2007). Lead removal from aqueous solution by natural and pretreated clinoptilolite adsorption equilibrium and kinetics, *J. Hazard Matter.* 146, 362-371
- Gil-Lim Y, Byung-Tak K, Baek-Oon K, Sang-Hun H. (2013) Chemical and Mechanical Characteristics of Crushed Oyster Shell. *Waste Management.* ;23: 825-834.

- Harish P. K. V., Tharanathan, R. N (2007). Chitin/Chitosan: Modifications and Their Unlimited Applications Potential- An Overview. *Trends in Food Science and Technology*, 18, 117-131
- Heet C., Gaurav D., Rushabh P., Maulin S., Anjali B., Sandeep R (2017). Synthesis and antimicrobial properties of chitosan: A Case Study. *EC Microbiology*, 9(5) 193-200
- Hobson, J.P (1969). Physical adsorption isotherms extending from ultrahigh vacuum to vapor pressure. *J. Phys. Chem.* 73, 2720–2727.
- Jimoh O.T, Muriana M, Izuelumba B (2011). Sorption of Lead (II) and Copper (II) ions from Aqueous Solution by Acid Modified and Unmodified Melina arboreal (Verbenaceae) leaves. *J. Emerg. Trends Eng. Appl. Sci.* 2(5):734 -740.
- Knight, C (2012). An alliance with Mother Nature: natural food, health and morality in low-carbohydrate diet books. *Food and Foodways*, 20: 102-122
- Langmuir, I., (1918). The Adsorption of Gases on Plane Surfaces of Glass, Mica, and Platinum. *J.A.M. Chem. Soc.*, 40: 1361-1403.
- Li, Q., Dunn, E. T., Grandmaison, E. W., Goosen, M. F. A (1992). Application and properties of chitosan. *J. Bioact. Compat. Pol.* 7, 370-397
- Malafaya, P.B., Silva, G., Reis, R. L (2007). Natural-Origin Polymers as Carriers and Scaffolds for Biomolecules and Cell Delivery in Tissue Engineering Applications. *Advanced Drug Delivery Reviews.* 59, 207-233
- Martins, A.F, Facchi, S.P, Follmann, H. D, Pereira, A.G, Rubira, A. F, Muniz, E. C (2014). Antimicrobial activity of chitosan derivatives containing N-quaternized moieties in its backbone: a review, *int.J.Mol.Sci.* 15, 20800-20832
- Musa, J. J (2010). Evaluating of the Lubricating Properties of Palm Oil. *Leonardo Electronic Journal of Practices and Technologies*, 79-84
- Ngo, D.A, Kim, S.K (2014). Antioxidant effects of chitin, chitosan, and their derivatives. In *Advances in Food and Nutrition Research*. Kim, S.K, Ed., Academic Press: Waotham, M. A, USA, vol. 73, 15-31
- Pawlak, A. & Mucha, M. 2003. Thermogravimetric and FTIR studies of chitosan blends. *Thermochimica Acta*, 396 (1–2), 153-166.
- Poku, K (2002). Small-scale Palm Oil Processing in Africa, *FAO Agricultural Services Bulletin*, 148: 1010-1365
- Randy C. F., Cheung, T. B. N., Jack H. W., Wai Y. C (2015). Chitosan: an uptake on potential biomedical and pharmaceutical applications. *Mar. Drugs* 13, 5156-5186
- Rinaudo, M (2006). Chitin and chitosan properties and applications. *Progress in Polymer Science.* (31) 7, 603-632
- Salawudeen T.O, Dada, E. O, Alagbe, S.O (2007). Performance evaluation of acid treated Clays for Palm Oil bleaching. *Journal Engineering and Applied Science.* 2; 1677-1680.
- Shanta Pokhrel, Paras Nath Yadsv, Rameshwar Adhikari (2015). Applications of Chitin and Chitosan in Industry and Medical Science: A Review. *Nepal journal of Science and Technology* 16 (1) 99-104

- Sorlier, P., A. Denuzière, C. Viton, and A. Domard (2001). "Relation between the Degree of Acetylation and the Electrostatic Properties of Chitin and Chitosan". *Biomacromolecules*, Vol. 2: 765–772.
- Tolamite, A., Desbrieres, J., Rhazi, M., Alagui, A., Vincendon, M., Vottero, P.,(2000). On the influence of deacetylation process on the physicochemical characteristics of chitosan from squid chitin. *Polymer*. 41, 2463-2469
- Tilahun M., Agegnehu A., Alemayehu M (2018). Comparison of physicochemical properties of edible vegetable oils commercially available in Bahir Dar, Ethiopia. *Chemistry International* 4(2) 130-135
- Temkin, M. J., Pyzhev, V., (1940). Kinetics of ammonia synthesis on promoted iron catalyts. *Acta Physiochim. Urss*, 12: 217-222.
- Tonfack Djikeng, F., Womeni, H.M., Kingne Kingne, F., Karuna, M.S.L., Rao, B.V.S.K., Prasad, R.B.N (2019). Effect of sunlight on the physicochemical properties of refined bleached and deodorized palm olein. *Food Research* 3 (1): 49 - 56
- Yerima, E. A., Yebpella, G. G., Ogah,E., Longbap,, D., Johson, S. N (2018). Effect of Extraction Methods on the Physicochemical Properties of Palm Kernel Oil. *Int. J. Modern Chem.* 10 (1): 104-116